J. Synchrotron Rad. (1999). **6**, 332–334

DAFS analysis of magnetite

Anatoly I. Frenkel,[a]*† Julie O. Cross,[b] David M. Fanning[a] and Ian K. Robinson[a]

[a]*University of Illinois at Urbana-Champaign, Urbana, IL 61801, USA,*
[b]*Naval Research Laboratory, Washington, D.C. 20375, USA.*
Email: frenkel@bnl.gov

The mechanism of the structural transformation in Fe_3O_4 during its Verwey transition at 120 K is not completely understood, partly due to the lack of knowledge of the details of the local structure around different Fe atoms in the unit cell. In our experiment, this information was obtained at room temperature using Diffraction Anomalous Fine Structure (DAFS) technique which has the ability to separately solve the local structures around the octahedral and tetrahedral sites in the spinel structure of magnetite. An iterative dispersion integral algorithm was used to isolate f' and f'' from the DAFS intensity and structural information was obtained from f'' using standard XAFS analysis methods. Relevance of our results to different models of Verwey transition is discussed.

Keywords: Diffraction anomalous fine-structure, magnetite, Verwey transition

1. Introduction

Magnetite (Fe_3O_4) exhibits a metal-insulator (Verwey) transition at 120 K which is accompanied by a structural transition at the same temperature. The low temperature structure and the mechanism of Verwey transition are not understood. Verwey, et al. [Verwey, 1947], proposed an ordering scheme in which alternative Fe^{2+} and Fe^{3+} ions exist along the *c*-axis in the lower symmetry structure. It has been recently suggested based on the results of neutron and electron diffuse scattering experiments that the low temperature structure is preserved locally in the high temperature phase up to at least 100 K above the transition temperature. Lack of consensus about the structure of magnetite at low temperature and the mechanism of Verwey transition is caused by the lack of accurate structural characterization of the low and high temperature phases.

X-ray absorption fine-structure (XAFS) technique is a perfect method, in many cases, to study the local structure around resonant (absorbing) atoms. However, XAFS analysis of magnetite is complicated due to the presence of crystallographically inequivalent (octahedral and tetrahedral) Fe sites in the unit cell. Diffraction Anomalous Fine Structure (DAFS), however, is a perfect technique to separate the different sites and independently solve the local structure around octahedral and tetrahedral Fe sites in magnetite.

As in the case of the "direct spinel" structure of Co_3O_4 first examined by DAFS [Pickering, 1993], two different Fe sites (octahedrally, Fe^{oct}, and tetrahedrally, Fe^{tetr}, coordinated) occur on high symmetry positions in the "inverse spinel" unit cell of Fe_3O_4. However, differently from the structure of Co_3O_4, the octahedral sites, Fe^{oct}, in Fe_3O_4 are populated by randomly substituting [Fe^{2+},Fe^{3+}] ions, whereas the tetrahedral sites, Fe^{tetr}, are populated by Fe^{3+} ions only. Therefore, they yield extra conditions for reflections above the basic space group (*Fd3m*) conditions. Hence, there are subsets of peaks for which only Fe^{oct} or only Fe^{tetr} atoms contribute, and another subset where both sites contribute to the crystallographic structure factor. For Fe^{oct} the most convenient for measurement is the (222) reflection, and for Fe^{tetr} both (022) and (224) are possible. For the site mixing case, the (444) reflection was used. The structure factors corresponding to all these reflections are purely real which is necessary for convergence of the data analysis algorithm.

DAFS signals at these 4 reflections were measured at room temperature and analyzed in this work. An iterative dispersion integral algorithm was used to isolate f' and f'' from the DAFS intensity. Structural information was obtained from f'' using standard XAFS analysis methods. Relevance of our results to various structural models of Verwey transition is discussed.

2. Experiment

Single crystal Fe_3O_4 was prepared by a modified Bridgman technique and oriented by Laue x-ray method. It was then cut into slices (ca. 1.5 × 1.5 mm^2 in area) by a diamond wafer saw and mechanically polished down to 150 μm thickness.

The DAFS experiment was performed at room temperature using a custom-designed 4-circle Kappa diffractometer at the National Synchrotron Light Source at Brookhaven National Laboratory, beamline X16C. Energy scans of (022), (224), (222) and (444) reflections were performed from 200 eV below to 1000 eV above the Fe *K* edge energy (7112 eV). The program SUPER was used for data collection, after suitable modification for energy-dispersive measurements. Fluorescence background was measured by repeating the DAFS scan after moving the phi motor of the diffractometer to an off-peak position.

Since $1s \rightarrow 4p$ transitions in Fe^{2+} and Fe^{3+} ions occur at different energies, precise absolute energy calibration is necessary during the scans in order to examine the *K* edge energy shifts. Simultaneous measurement of absorption through the sample and the reference foil placed directly downstream to the sample is one of the most commonly used energy calibration methods in transmission XAFS experiments, which, obviously, cannot be used in Θ - 2Θ diffraction geometry. To calibrate energy, we used air-scattered radiation and monitored its absorption in a reference Fe foil, as described in [Cross, 1998].

3. Processing DAFS data

Background subtracted, I_0 – normalized DAFS data for different reflections are shown in Fig. 1 in the vicinity of the Fe *K* absorption edge energy. Visual inspection of the data yields the following immediate conclusions:

† Mailing address: Building 510 E, Brookhaven National Laboratory, Upton, NY 11973, USA

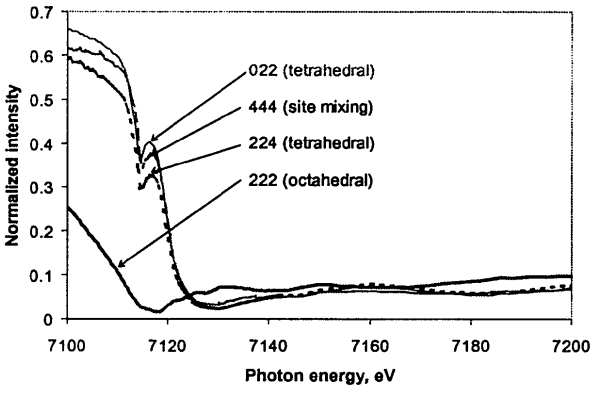

Figure 1
Background subtracted, I_0-normalized Bragg intensity vs. energy for different reflections in magnetite.

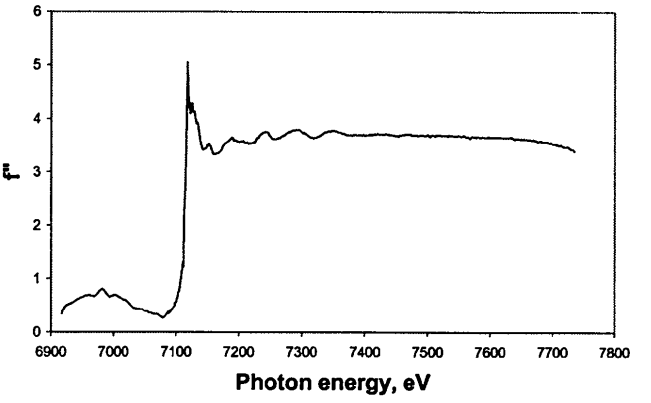

Figure 2
Resonant scattering amplitude *f''(E)* for (222) Bragg reflection with contributions of octahedrally coordinated Fe atoms only (as well as oxygens).

1. The peak in the near edge region (between 7110 and 7120 eV) in (022), (224) and (444) DAFS data is described in literature as evidence of the $1s \rightarrow 3d$ transition. This dipole-forbidden transition is pronounced in the above reflections due to the contribution of the tetrahedral sites where metal *4p* and oxygen *2p* are mixed with t_2 *d* orbitals. Alternately, for the octahedral sites, the $1s \rightarrow 3d$ transition amplitude is weak in O_h symmetry, explaining the featureless behavior of the (222) DAFS signal in the near edge region.

2. Large energy shift towards lower energies is apparent in the onset of the $1s \rightarrow 4p$ transition for the (222) reflection DAFS signal relative to that in other data sets. Careful examination of the site-mixing (444) reflection DAFS data yields a much smaller energy shift in the same direction. In both cases, these shifts are the evidence of the presence of Fe^{2+} in the structure factors corresponding to both the (222) and (444) reflections and the presence of only Fe^{3+} in both (022) and (224) reflections. The chemical shift between Fe^{2+} and Fe^{3+} ions is expected to be as large as 5 eV [Toyoda, 1997]. In our case, the quantitative attribution of the $1s \rightarrow 4p$ transition energy for each reflection is possible after separating *f'* and *f''* from the Bragg intensity data.

An iterative dispersion integral algorithm was used to isolate *f'* and *f''* from the Bragg intensity as described in [Cross, 1996]. *f''(E)* is related to the absorption cross section by the optical theorem, and XAFS data analysis methods, described in the next Section, are directly applicable to *f''(E)* after pre-edge removal, background subtraction and normalization.

4. Local structure around octahedrally coordinated Fe atoms

Local structure around octahedrally coordinated Fe atoms was obtained using the *f''(E)* (Fig. 2) extracted from the (222) reflection DAFS data (Fig. 1). Data analysis was performed using UWXAFS package [Stern, 1995] in three steps:

1. Smooth atomic background function was removed using AUTOBK code and the normalized EXAFS $\chi(k)$ was obtained (Fig. 3).

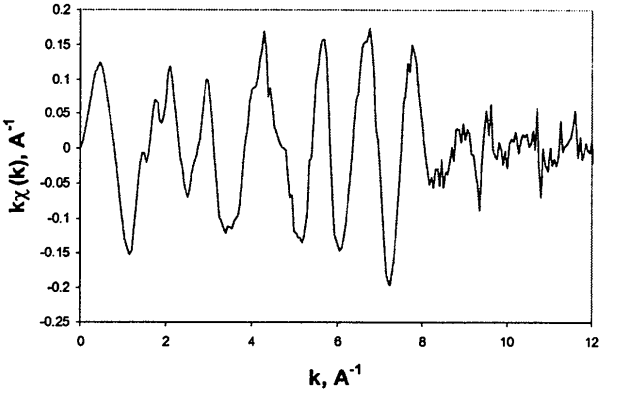

Figure 3
Background subtracted and normalized, *k*-weighted EXAFS function $\chi(k)$ obtained from *f''(E)* for the (222) reflection (Fig. 2) and generated by the octahedrally coordinated absorbing Fe atoms only.

2. Theoretical $\chi(k)$ was constructed using FEFF6 code [Zabinsky, 1995]. In the model, absorbing atoms were octahedrally coordinated Fe atoms only.

3. FEFF6 theory was fitted to the data in *r*-space using FEFFIT code. Two nearest neighbor shells were included in the theoretical calculation: Fe^{oct} – O (where Fe^{oct} denotes octahedrally coordinated [Fe^{2+},Fe^{3+}] ions and O denotes oxygen atoms forming the FeO_6 octahedron) and Fe^{oct} - Fe^{oct} (distance between the centers of the adjacent FeO_6 octahedra). These shells contribute to the first two peaks in the Fourier transform magnitude of $k\chi(k)$ between 1.3 and 3 Å (Fig. 4). More distant Fe^{oct} – Fe^{tetr} (i.e., Fe^{3+}) neighbors contribute to the shoulder between 3 and 3.5 Å (Fig. 4; see also [Harris, 1998]) and are not included in the analysis. 6 variables were adjusted in the fit: S_0^2, ΔE_0 (O), ΔE_0 (Fe), σ^2(Fe-O), σ^2(Fe-Fe), and ε (isotropic lattice expansion). The number of relevant independent data was 8.

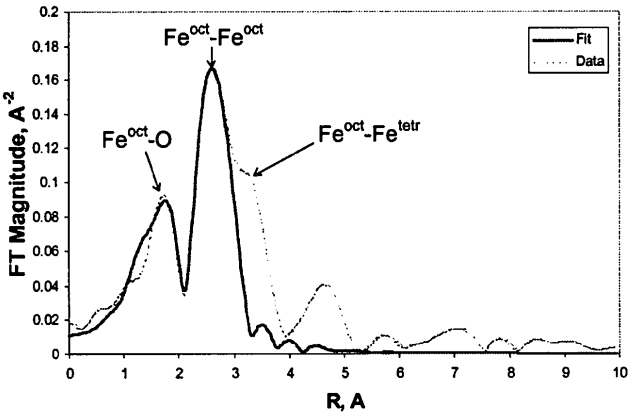

Figure 4
Fourier transform magnitudes of experimental data and fit with FEFF6 theory for $k\chi(k)$, where absorbing atoms are octahedrally coordinated Fe atoms only.

Fit results for bond distances and their mean square disorder are summarized in Table 1. The best-fit result for ε = 0.004 ± 0.008 attests the reliability of our procedure: the corresponding bond lengths (Table 1) differ only by 0.01 from the published values. Unrealistically low value obtained for S_0^2 (0.30 ± 0.08) is an evidence of strong self-absorption which was not completely corrected for in the process of DAFS data reduction. This correction acts upon $\chi(k)$ as a constant factor and does not affect, therefore, our structural results.

Table 1
Bond distances and their mean square disorder obtained for the nearest neigbors to the octahedrally coordinated Fe atoms.

Bond	R, Å	σ^2, Å^2
Fe^{oct}-O	2.07 ± 0.01	0.017 ± 0.008
Fe^{oct}-Fe^{oct}	2.98 ± 0.01	0.0005 ± 0.003

Enhanced disorder in Fe^{oct} – O bonds (0.017 ± 0.008 Å^2) compared to the relatively low disorder in Fe^{oct} - Fe^{oct} pair lengths (Table 1) is intriguing. One possible explanation is that modeling Fe^{oct} - O interactions using a perfectly rigid FeO_6 octahedron is a poor approximation not taking into account that both Fe^{2+} and Fe^{3+} ions (with different Fe – O bond lengths) populate the octahedral sites in dynamic equilibrium. This enhanced disorder is also consistent with the molecular polaron model [Yamada, 1980]. To verify these and other models, simultaneous analysis of two $\chi(k)$ data sets (obtained for tetrahedrally and octahedrally coordinated Fe atoms from either (022) or (224) reflections, and from (222) reflection, respectively) seems to be necessary.

5. Conclusions

DAFS measurements were performed in magnetite at several Bragg reflections which made it possible to separately solve the local structure around octahedrally and tetrahedrally coordinated Fe atoms.

These experiments also enabled us to discriminate $1s \rightarrow 3d$ and $1s \rightarrow 4p$ electronic transitions between Fe^{2+} and Fe^{3+} ions in magnetite.

Local structure around octahedrally coordinated Fe^{oct} atoms was solved using the $f''(E)$ extracted from the (222) reflection DAFS data. Nearest neighbor distances and their disorder were obtained for the Fe^{oct} - O and Fe^{oct} - Fe^{oct} pairs.

Disorder in Fe^{oct} – O bonds was found to be larger than expected in a rigid octahedron. More studies are necessary to identify the origin of this enhanced disorder.

We thank Prof. F. A. Chudnovsky for many useful discussions and Dr. P. A. Metcalf for sample preparation. This work was supported by the DOE Grant No. DEFG02-96ER45439 through the Materials Research Laboratory at the University of Illinois at Urbana-Champaign.

References

Cross, J. O. (1996). Ph. D. Thesis, University of Washington, Seattle.

Cross, J. O. & Frenkel, A. I.. Rev. Sci. Instrum., in press.

Harris, V. G., Koon, N. C., Williams, C. M., Zhang, Q., Abe, M. & Kirkland, J. P. (1996). Appl. Phys. Lett., **68**, 2082.

Pickering, I. J., Sansone, M., Marsch, J., & George, G. N. (1993). J. Am. Chem. Soc., **115**, 6203.

Stern, E. A., Newville, M., Ravel, B., Yacoby, Y. & Haskel, D. (1995). Physica B, **208 & 209**, 117.

Toyoda, T., Sasaki, S. & Tanaka, M. (1997). Jpn. J. Appl. Phys., **36**, Pt. 1, 2247.

Verwey, E. J. W., Haayman, P. W. & Romeijn, F. C. (1947). J. Chem. Phys., **15**, 181.

Yamada, Y., Wakabayashi, N. & Nicklow, R. M. (1980). Phys. Rev. B, **21**, 4642.

Zabinsky, S. I., Rehr, J. J., Ankudinov, A., Albers, R. C., & Eller, M. J. (1995). Phys. Rev. B, **52**, 2995.

(Received 10 August 1998; accepted 19 October 1998)